Homeodomain protein Sxi1α regulates cell-cell fusion during distinct sexual reproduction modes in *Cryptococcus deneoformans*

Jun Huang, Patricia P. Peterson, Ziyan Xu, Liping Xiong, Sheng Sun, and Joseph Heitman*

Department of Molecular Genetics and Microbiology, Duke University Medical Center, Durham, NC 27710, USA

* Corresponding author: Joseph Heitman
Email: heitm001@duke.edu
Keywords: Homeodomain protein; Cell-cell fusion; Unisexual reproduction.

Abstract

Sex-specific homeodomain (*HD*) proteins are key regulators of cell identity and sexual development in fungi, typically functioning as heterodimers to regulate transcription. In the human fungal pathogens *Cryptococcus neoformans* and *Cryptococcus deneoformans*, the *HD* proteins Sxi1α and Sxi2**a** (sex-induced 1α and 2**a**) have been characterized as interacting partners that play critical roles in sexual development during **a** x α sexual reproduction. Given the dominance of α cells in natural populations of *Cryptococcus*, the roles of Sxi1α and Sxi2**a** in unisexual reproduction, which predominantly involves same-sex (α x α) mating, remain unclear. To elucidate the functions of Sxi1α and Sxi2**a** in unisexual reproduction, we first used AlphaFold3 to predict their structures, which revealed the potential for both heterodimeric and homodimeric complexes. We subsequently deleted *SXI1*α and *SXI2***a** in the hyperfilamentous self-fertile *C. deneoformans* strains XL280**a** and XL280α. Disruption of these genes did not result in noticeable defects in vegetative growth, virulence-associated traits, colony morphology, sporulation, or competitiveness during either **a** x α or α x α crosses. Surprisingly, the absence of *SXI1*α significantly increased the cell–cell fusion rate during both α x α and **a** x α mating, suggesting a novel inhibitory role for Sxi1α, independent of the partner Sxi2**a**. Together, our findings revealed an unexpected function of Sxi1α in regulating cell fusion, which may contribute to the predominance of *MAT*α isolates in global *Cryptococcus* populations and the conservation of *SXI1*α in a population that is predominantly α mating type.

Introduction

Sexual reproduction is a key process in eukaryotic organisms, promoting genetic diversity and facilitating adaptation under changing environments. In fungi, this process is controlled by the mating-type (*MAT*) locus, a specific genomic region containing genes required for successful mating. Among these genes, pheromone and pheromone receptors (*P/R*) are involved in signal transduction and recognition between mating partners, and homeodomain (*HD*) transcription factors act as master regulators that control the expression of genes necessary for sexual development (Yadav et al. 2023). In the model yeast *Saccharomyces cerevisiae*, Mat**a**1 and Matα2 are well-characterized HD proteins, forming heterodimers that bind DNA cooperatively to repress transcription of cell type-specific genes (Goutte and Johnson 1988; Li et al. 1995). Unlike *MAT***a**1,which promotes **a**-specific gene expression, *MAT*α2 can form homodimers to repress **a**-specific genes (Keleher et al. 1988; Herskowitz 1989; Goutte and Johnson 1993). In the corn smut fungus *Ustilago maydis*, HD proteins bWest (bW) and bEast (bE) dimerize to regulate fungal morphological switching, and interactions with the plant hosts (Gillissen et al. 1992; Kämper et al. 1995; Wahl et al. 2010; Vollmeister et al. 2012). Similarly, sexual development in the mushroom *Coprinus cinereus* requires the physical interaction of two HD proteins, HD1 and HD2 (Kües et al. 1994).

In the human fungal pathogens *Cryptococcus neoformans* (formerly *C. neoformans* var. *grubii*, serotype A) and its sister species *C. deneoformans* (formerly *C. neoformans* var. *neoformans,* serotype D*)*, the *P/R* and *HD* genes as well as additional genes reside in a relatively large (>100 kb) *MAT* locus (Hull et al. 2005; Sun, Coelho, et al. 2019; Bian et al. 2024). In addition to its role sexual reproduction, the *MAT* locus has been associated with several non-mating functions in *Cryptococcus*, including fungal virulence and uniparental mitochondrial inheritance (mito-UPI), in which mitochondrial DNA is predominantly inherited from the *MAT***a** parent after a x α sexual reproduction. (Kwon-Chung and Bennett 1978; Yan et al. 2004). We previously identified the *Cryptococcus* sex-specific HD proteins Sxi1α (Sex inducer 1α) and Sxi2**a** (Sex inducer 2**a**), which heterodimerize and are involved in cell identify, sexual development, and mito-UPI during **a** x α bisexual reproduction, with evidence indicating that, beyond Sxi1α and Sxi2**a** , the *P/R* locus is involved in mito-UPI process as well. (Hull et al. 2002; Hull et al. 2004; Yan et al. 2004; Yan et al. 2004; Hull et al. 2005; Sun et al. 2020). Several conserve and novel

73 downstream targets (e.g., *CLP1* (clampless 1) and *CPR2* (*Cryptococcus* pheromone receptor 2)) of Sxi1α
74 and Sxi2**a** involved in sexual reproduction have been identified (Ekena et al. 2008; Hsueh et al. 2009;
75 Heimel et al. 2010; Mead et al. 2015). Additional evidence suggests that Sxi1α is not required for
76 virulence in *C. neoformans* (Hull et al. 2004) and the role of Sxi2**a** in virulence remains unclear. In
77 addition to **a** x α bisexual reproduction, unisexual reproduction can also occur between partners of the
78 same mating type (mainly α x α) in *C. neoformans* and *C. deneoformans* (Lin et al. 2005). In natural
79 *Cryptococcus* populations, *MAT*α isolates are predominant among both clinical and environmental
80 samples, suggesting that **a** x α heterothallic sexual reproduction is infrequent (Kwon-Chung and Bennett
81 1978; Desjardins et al. 2017). This strong bias in *MAT* locus distribution may, at least in part, be explained
82 by the occurrence of unisexual reproduction, which enables genetic recombination and propagation in the
83 absence of a compatible mating partner (Lin et al. 2005; Sun et al. 2014; Roth et al. 2018). As key sex-
84 specific transcriptional regulators, the roles of Sxi1α and Sxi2**a** in unisexual reproduction remain to be
85 elucidated.

86 In this study, we sought to determine whether Sxi1α and Sxi2**a** are involved in same-sex mating
87 in *Cryptococcus*. Protein prediction via AlphaFold3 suggested that Sxi1α and Sxi2**a** can dimerize and
88 potentially form both heterodimer as well as homodimers. Taking advantage of the hyperfilamentous *C.*
89 *deneoformans* congenic isolates XL280α and XL280**a**, along with the CRISPR/Cas9 gene editing system,
90 we deleted *SXI1*α and *SXI2***a** in XL280α and XL280**a**, respectively. Consistent with previous results, we
91 found that *SXI1*α and *SXI2***a** are dispensable for vegetative growth and multiple virulence factors,
92 including thermotolerance at 37°C, polysaccharide capsule formation, and melanin production.
93 Interestingly, no obvious defects in colony morphology, hyphal development, basidium formation,
94 sporulation, spore germination or competitiveness were detected in *sxi1*αΔ or *sxi2***a**Δ mutants during
95 unisexual reproduction. In contrast, we found that Sxi1αΔ with significantly increased cell-cell fusion
96 frequency during both α x α and **a** x α crosses. Overall, our results suggest a novel function of Sxi1α in
97 regulating cell-cell fusion, which may influence the sexual reproduction in global populations of
98 *Cryptococcus*.

99

Materials and methods

Fungal strains and growth conditions

C. deneoformans and *C. neoformans* strains for this study are listed in Table S1. The strains were stored in 15% glycerol at -80°C for long-term storage. Fresh strains were streaked from glycerol stock and maintained on solid YPD medium (1% yeast extract, 2% Bacto Peptone, 2% dextrose) at 30°C.

Spot dilution assays were performed with overnight cultures of the tested strains grown in liquid YPD at 30°C. Strains were diluted to an OD_{600} of 0.5 in sterile water. These cultures were further serially diluted 5-fold and spotted (3 µL for each dilution) onto YPD plates. The plates were incubated at 30°C and 37°C (testing thermotolerance) for 2 days before imaging.

Protein structural predictions

Protein structure predictions were made with AlphaFold3 (Abramson et al. 2024) on the AlphaFold server (https://alphafoldserver.com/). The predicted models and error plots were further processed with Chimera X (v 1.9) (Meng et al. 2023) for predicted local distance difference test (pLDDT) value filtering, alignment, and visualization.

Gene deletion and confirmation

Approximately 1.0 kb 5' and 3' flanking regions of *SXI1*α and 60 bp 5' and 3' flanking regions of *SXI2***a** were constructed using primers listed in Table S2 to target their respective genes for homologous recombination. Overlap PCR with a selectable marker was used to construct the DNA donor with 1.0 kb homology, while 60 bp microhomology was included in the primers for donor amplification. *C. neoformans* codon optimized Cas9, gRNAs (a single gRNA targeting *SXI1*α and two gRNAs targeting *SXI2***a**), and drug resistance cassettes (*NAT* from pAI3 or *NEO* from pJAF1) containing homologous flanking sequences were introduced into XL280 wild-type strains via the previously reported Transient CRISPR-Cas9 Coupled with Electroporation (TRACE) system (Fan and Lin 2018; M.Y. Huang et al. 2022). Transformants were screened using internal PCR to the ORF, and 5′ and 3′ junction PCR to the drug resistance maker to confirm integration at the genomic locus. Illumina whole-genome sequencing was performed on positive transformants using Novaseq X Plus platform (2x150 bp). The sequencing reads

were mapped to a modified version of the XL280α genome (Fu et al. 2021) with Burrows-Wheeler Alignment tool (BWA) (v 0.7.17) (Li and Durbin 2009) to further confirm the deletion mutant strains. The modification included adding the *MAT***a** locus sequence of JEC20 (GenBank: AF542530.2) as an additional contig.

Capsule formation and melanin production assays

Tested strains, with an initial OD_{600} of 0.1 in 4 mL liquid RPMI medium (RPMI 1640 with 2% dextrose), were incubated on a roller drum at 70 rpm and 30°C for 3 days. After washing and resuspension in water, the cells were negatively stained with an equal volume of India ink to visualize the capsules.

To assess melanin production, overnight saturated cultures of test strains were spotted (10 μL) onto Niger seed agar plates (7% Niger seed, 0.1% dextrose). The Niger seed plates were incubated at 30°C and 37°C for 8 days before photographing.

Competition assays

Overnight cultures of tested strains grown in liquid YPD at 30°C were diluted to OD_{600} of 0.2 and equally mixed in a 1:1 ratio in 5 mL of liquid YPD for co-culture. *sxi1*αΔ::*NAT* mutants (resistant to NAT) and *sxi2***a**Δ::*NEO* mutants (resistant to G418) were mixed with XL280α and XL280**a**, respectively. The mixture was plated on YPD plates, YPD + nourseothricin (NAT), and YPD + neomycin (G418) to confirm starting ratio. After 24 and 48 hours of co-culture, an aliquot of the mixture was sampled and plating was repeated with OD_{600} diluted to 0.1 to track changes in relative abundance of mutants. Four independent replicates were performed for each competition.

For the competition assay performed on MS medium, overnight cultures were similarly diluted to OD_{600} of 1. *sxi1*αΔ::*NAT* or *sxi2***a**Δ::*NEO* mutants and the corresponding XL280 wildtype strain were equally mixed in a 1:1 ratio and spotted on MS medium. Spores were dissected 10 to 14 days post spotting. Yeast cells from internal regions were also collected. Spores or yeast cells were further transferred to YPD+NAT, YPD+G418 and YPD to determine the ratio of mutants in the population. Five independent spots were investigated for each competition.

Mating and cell-cell fusion assay

Mating plates were set up as described previously (Sun, Priest, et al. 2019). α x α unisexual and **a** x α sexual reproduction assays were performed on Murashige and Skoog (MS, Sigma, USA) plates for 1 to 2 weeks before imaging and dissection. Basidiospores generated during unisexual reproduction were randomly dissected and plated on YPD plates for 2 to 3 days to determine spore viability and germination rates.

Cell-cell fusion frequency during α x α unisexual outcrossing in XL280α *NAT* (XL561 and XL562) and XL280α *NEO* (XL563 and XL564) was compared to bilateral mutant crosses of *sxi1*αΔ::*NAT* and *sxi1*αΔ: *NEO* or the unilateral crosses of *sxi1*αΔ::*NAT* and XL280α *NEO*. Additionally, XL280α *NAT* (XL561) and XL280**a** *NEO* (JHG223) were used as wildtype strains to test the role of *SXI1*α and *SXI2***a** in cell-cell fusion during **a** x α sexual reproduction. Both bilateral (*sxi1*αΔ::*NAT* x *sxi2***a**Δ::*NEO*) and unilateral crosses (*sxi1*αΔ::*NAT* x XL280**a** *NEO* and XL280α *NAT* x *sxi2***a**Δ::*NEO*) were analyzed.

Cells were diluted in sterile water to an OD_{600} of 1. Two *MAT*α strains (α x α outcrossing) containing either *NAT* or *NEO* resistance cassettes were mixed equally with JEC20 (*MAT***a**) for assisted mating on V8 agar (pH = 7.0) and incubated for 72 hours in the dark at room temperature. For **a** x α crossing, cells were prepared similarly but without adding additional JEC20 on V8 agar (pH = 7.0) and incubated for 48 hours in the dark at room temperature. The cells were then collected and plated on YPD + NAT + G418 and YPD alone to determine the ratio of colonies with dual resistance 4 to 5 days post-plating (i.e., fusion product) out of the total cells. It should be noted that when screening for fusion products from crosses between XL280**a** *NEO* and XL280α *NAT* on YPD+NAT+G418 rich medium plates, we observed that in addition to colonies formed by yeast cells, there were also tiny colonies that produced extensive hyphae with occasional formation of basidia and basidiospore chains. It is not yet clear what is the nature of these highly filamentous colonies, and thus, in the current analysis we only included yeast-like colonies for clarity.

Light and scanning electron microscopy (SEM)

Mating structures from MS plates were imaged with an AxioSkop 2 fluorescence microscope to visualize hyphae, basidia and basidiospores under brightfield. SEM samples were prepared following a

previously described protocol (Peterson et al., 2024), with minor modifications. Briefly, a ~2 cm × 2 cm agar plug containing patch of mated cells from MS plates was fixed in PBS containing 4% formaldehyde and 2% glutaraldehyde at 4°C for 2 hours. The fixed samples were then gradually dehydrated in a graded ethanol series (30%, 50%, 70%, 95%), with each step performed at 4°C for 15 min. This was followed by three washes in 100% ethanol, each at 4°C for 15 min. The samples were further dehydrated using a Ladd CPD3 Critical Point Dryer and subsequently coated with a thin layer of gold with a Denton Desk V Sputter Coater (Denton Vacuum, USA). Hyphae, basidia and basidiospores were observed with a scanning electron microscope equipped with an EDS detector (Apreo S, ThermoFisher, USA).

Statistical analysis

Paired or unpaired student t-tests were performed in Rstudio (version 2024.04.1+748) using the “t.test” function with argument “paired = TRUE” for paired tests or “paired = FALSE” for unpaired tests.

Results and Discussion

Sxi1α and Sxi2a are predicted to form a heterodimer

To study the impacts of the homeodomain proteins Sxi1α and Sxi2**a** on unisexual reproduction in *Cryptococcus*, we selected to study XL280α and XL280**a**, a pair of congenic strains of *C. deneoformans*, that are well-known for the ability to undergo unisexual reproduction which exhibit robust self-filamentation and sporulation (Lin et al. 2005; Zhai et al. 2013). Sxi1α and Sxi2**a** are conserved between *C. neoformans* and *C. deneoformans*, and homeodomain (Pfam:00046) or homeobox KN domains (from **KN**OX family transcription factors, Pfam:PF05920) were found within the sequences via NCBI conserved domain search (Figure 1A). Both domains are structurally related, sharing DNA-binding functions through a helix-turn-helix motif, suggesting potential functional relevance in regulating gene expression. Similar to our previous report with yeast two-hybrid analysis (Hull et al. 2002; Hull et al. 2005), a heterodimer between Sxi1α and Sxi2**a** was predicted by AlphaFold3 protein-protein complex prediction (Figure 1B). Pairwise structural alignments between the predicted Sxi1α-Sxi2**a** heterodimer and the crystal structure of the *S. cerevisiae* MAT**a**1-MATα2 heterodimer (Li 1998) revealed robust structural similarity between the two homeodomain complexes with an RMSD value of 0.561 angstroms between 49 pruned atom pairs (Figure 1C). Similarly, the Sxi1α-Sxi2**a** heterodimer exhibited high structural similarity to the AlphaFold3-predicted bW-bE heterodimer from the corn smut fungus *Ustilago maydis*, with a RMSD of 1.069 angstroms across 40 pruned atom pairs, supporting a conserved structure for the *MAT* locus-specific HD complex in fungi.

Previous studies showed that, in addition to forming a heterodimer with MAT**a**1, *S. cerevisiae* MATα2 forms a homodimer to repress **a**-specific genes (Dranginis 1990). Therefore, we tested whether Sxi1α and Sxi2**a** can also form homodimers. AlaphaFold3 predicted the potential formation of a low-confidence homodimer of Sxi1α-Sxi1α (ipTM = 0.14 pTM = 0.23) and of Sxi2**a**-Sxi2**a** (ipTM = 0.2 pTM = 0.24) (Figure 1D). These predictions suggest weak interactions, and further experimental validation is required to confirm if these may have biological relevance.

Sxi1α and Sxi2a are dispensable for *in vitro* growth and virulence traits

To further characterize the phenotypic impacts of Sxi1α and Sxi2**a**, we deleted *SXI1*α and *SXI2***a** genes in XL280α and XL280**a**, respectively, with a CRISPR/Cas9-based strategy. In combination with a previously established TRACE electroporation protocol (Fan and Lin 2018; M.Y. Huang et al. 2022), several drug-resistant transformants (4 for XL280α *sxi1*αΔ::*NAT* and 2 for XL280**a** *sxi2***a**Δ::*NEO*) were confirmed with correct genotypes as deletion mutants based on 5' junction, 3' junction, and ORF specific PCR analysis (Figure 2A). Mapping of reads generated from Illumina whole-genome sequencing further confirmed the complete deletion of the genes in all four *sxi1*αΔ mutants and one of the two *sxi2***a**Δ mutants, and a partial gene deletion in the other *sxi2***a**Δ mutant. (Figure 2B). Interestingly, in some of the mutants elevated read-depth were observed in the flanking regions used for homologous recombination during gene deletion, indicating a potential concatemeric or ectopic insertion (J. Huang et al. 2022) of the resistance cassette (Figure 2B).

We next performed competition assays to assess the impact of Sxi1α and Sxi2**a** on fungal fitness during vegetative growth. Equal amounts of mutant and wildtype cells were mixed in liquid YPD and incubated at 30°C to assess the population dynamics. All of the tested *sxi1*αΔ and *sxi2***a**Δ deletion strains showed similar fitness compared to their respective wildtype strains after 24h or 48h of incubation compared to the initial starting proportion (0h), and thus the mutations confer no fitness defect (Figure 2C). Additionally, we characterized the contributions of Sxi1α and Sxi2**a** to several major virulence traits: thermotolerance at 37°C, capsule formation, and melanin production. Consistent with our previous reports in *C. neoformans* (Hull et al. 2004), none of the *sxi1*αΔ or *sxi2***a**Δ deletion strains displayed altered virulence traits compared to the XL280 wildtype strains (Figure 2, D-F). Taken together, these results indicate that the loss of *SXI1*α and *SXI2***a** does not affect the fitness of the XL280 strain during vegetative growth and has no impact on virulence-related traits.

Sxi1α and Sxi2a are dispensable for morphology, sporulation and cell viability during unisexual reproduction

We next investigated whether Sxi1α and Sxi2**a** are involved in unisexual reproduction in the XL280 background. When grown on mating and selfing inducing MS solid medium (Xue et al. 2007) as

252 solo-cultures, all of the tested *sxi1*αΔ and *sxi2***a**Δ mutants were able to produce elongated hyphae as well
253 as basidia and basidiospore chains at levels similar to their of XL280 wildtype controls (Figure 3, A-B),
254 with no discernable differences of basidium and basidiospores observed by scanning electron microscope
255 (SEM) (Figure 3C). Thus, the deletion of *SXI1*α and *SXI2***a** did not affect unisexual reproduction
256 morphologically. Additionally, we collected random meiotic basidiospores by microdissection to test the
257 effect of Sxi1α and Sxi2**a** on spore germination rates and cell viability and found no significant difference
258 in germination rates between spores produced by the *sxi1*αΔ mutants and XL280α (p-values: 0.6477 (Δ#4
259 vs XL280α) and 0.1788 (Δ#5 vs XL280α), unpaired t-test), as well as between spores produced by the
260 *sxi2***a**Δ mutants and XL280**a** (p-values 0.59 (Δ#6 vs XL280**a**:) and 0.7498 (Δ#7 vs XL280**a**), unpaired t-
261 test) (Figure 3D).

262 We previously observed that strains capable of undergoing unisexual reproduction exhibit higher
263 competitiveness than mutants with unisexual reproduction defects, attributing to enhanced hyphal growth
264 and sporulation (Phadke et al. 2013). To this end, for each deletion strain we mixed equal numbers of
265 cells from the mutant (containing dominant drug-resistant marker) and its wildtype control strain (sensitive
266 to drug), and spotted the mixture on MS medium to induce unisexual reproduction. After robust
267 sporulation was observed, we dissected two populations: 1) random basidiospores from the periphery
268 where sporulation occurs, and 2) the center of the spot where cells remain mostly as yeast (Figure 3E, left
269 panel). After the germination of the dissected spores/yeast cells, we transferred them onto YPD plates
270 containing selective drug (i.e., NAT or G418) to determine from which strain in the mixture did they
271 originate from. We found that for both Sxi1α and Sxi2**a**, the ratios between mutant and wildtype among
272 the basidiospores at the periphery were similar to those among the yeast cells at the center
273 (spores/yeast, p-values: 0.5398275 (*sxi1*αΔ) and 0.379667 (*sxi2***a**Δ), paired t-test), indicating the loss of
274 Sxi1α and Sxi2**a** did not affect fungal competitiveness during unisexual reproduction (Figure 3E, right
275 panel).
276
277 **Sxi1α is critical for cell-cell fusion**
278 In the presence of a helper strain serving as a pheromone donor, α x α outcrossing can be
279 facilitated in *C. deneoformans* in so called Ménage à trois matings (Hull et al. 2002; Lin et al. 2005).

Previously, our results from **a** x α sexual reproduction suggested that Sxi1α and Sxi2a function after cell-cell fusion (Hull et al. 2005). Although cell-cell fusion is dispensable for unisexual reproduction, it may still occur under certain conditions, such as during α x α outcrossing (Hull et al. 2002; Lin et al. 2005). Given the limited understanding of Sxi1α's role in this context, we sought to determine whether Sxi1α is involved in cell-cell fusion during α-α outcrossing. In the presence of a helper strain (JEC20, *MAT***a** *NAT*^{S} *NEO*^{S}), equal numbers of cells from strains XL280α and *sxi1*αΔ that were differentially resistant to *NAT* and *NEO* were mixed (*SXI1*α x *SXI1*αΔ, *SXI1*α x *sxi1*αΔ, and *sxi1*αΔ x *sxi1*αΔ) and spotted on V8 agar (pH=7.0) to induce sexual reproduction. After 72 hours of incubation, cells were collected. We found fusion frequency fewer than 5.04x10^{-8} in two independent of the XL280α *NAT* x XL280α *NEO* crosses, identified by screening colonies for double resistance to NAT and G418. In contrast, significantly higher fusion frequencies were found in *sxi1*αΔ::*NAT* x *sxi1*αΔ::*NEO* (22-fold higher than wildtype, frequency: 1.13x10^{-6}, p-value:0.00, unpaired t-test) and *sxi1*αΔ::*NAT* x XL280α *NEO* (62-fold higher than wildtype, frequency: 3.17x10^{-6}, p-value: 0.0080, unpaired t-test) (Figure 3F). Taken together, our results demonstrated that cell-cell fusion between *MAT*α cells significantly increased when the *SXI1*α gene was absent in at least one of the two strains.

We then asked whether Sxi1α, and possibly Sxi2**a** as well, have similar effects on cell-cell fusion during **a** **x** α bisexual mating. Surprisingly, we found that *sxi1*αΔ x wildtype unilateral (2.3-fold higher than wildtype, frequency:9.47x10^{-5}) and *sxi1*αΔ x *sxi2***a**Δ bilateral crosses (5.7-fold higher than wildtype, frequency: 2.31x10^{-4}) exhibited significantly higher **a** x α cell fusion frequency than XL280 wildtype crosses (frequency:4.04x10^{-5}) (p-value: 0.0273 (vs unilateral cross) and 0.0259 (vs bilateral cross) of unpaired t-test) (Figure 3G). Interestingly, the fusion frequency of *sxi2***a**Δ unilateral crosses was similar to the wildtype crosses (frequency:3.12x10^{-5}) (p-value: 0.2613 of unpaired t-test) (Figure 3G).

Previously, we found that the **a** x α cell fusion frequency in bilateral or unilateral crosses of *sxi1*αΔ and *sxi2***a**Δ deletion strains in the auxotrophic background of *C. deneoformans* was 1.5- to 1.9-fold higher than that of wildtype **a** x α fusion (Hull et al. 2005). This finding supports a role of Sxi1α in inhibiting **a** x α fusion, but the differing properties of Sxi2**a** across experiments remains unclear. A possible explanation could be that a of background α x α fusion in XL280 might influence **a** x α fusion frequency, reducing the detectable difference between wildtype and mutant strains.

The AlphaFold3-predicted heterodimer structure of Sxi1α and Sxi2**a** closely resembles the yeast MAT**a**1-MATα2 complex (Li 1998) and the predicted *U. maydis* bW-bE heterodimer, consistent with prior studies (Hull et al. 2002; Hull et al. 2005). This supports the importance of the Sxi1α-Sxi2**a** complex in **a** x α mating. Additionally, lower-confidence predictions suggest that Sxi1α and Sxi2**a** may form homodimers, indicating potential independent roles before cell-cell fusion.

In the absence of Sxi1α and/or Sxi2**a**, **a** x α mating is severely impaired, as indicated by the absence of normal hyphae during **a** x α sexual reproduction in the *C. neoformans* reference strain H99 and the C. *deneoformans* strains JEC43 and JEC34 (Hull et al. 2002; Hull et al. 2005). However, in our study, we found that the disruption of Sxi1α or Sxi2**a** does not affect the mating morphology and sporulation of the strain XL280 during unisexual reproduction, suggesting that these factors may play distinct roles in α x α versus **a** x α reproduction. The inhibitory role of Sxi1α we identified in cell-cell fusion is unexpected, partly because previous studies concluded that Sxi1α functions post-cell fusion (Hull et al. 2002; Hull et al. 2005). Because Sxi1α inhibits cell-cell fusion, it may reduce the efficiency of α cells participating in sexual reproduction. Given the predominance of *MAT*α isolates in natural populations, Sxi1α and Sxi2**a** likely have additional roles beyond **a** x α mating. Over evolutionary time, this reduced mating potential could contribute to the widespread dominance of *MAT*α strains by selecting alternative reproductive strategies or favoring unisexual reproduction. Interestingly, by analyzing the 341 *MATα* clinical and environmental isolates in the *C. neoformans* Strain Diversity Collection (Desjardins et al. 2017) through a similar pipeline as reported in our previous work (Huang et al. 2024; Martínez and Magwene), we found there were only two closely related environmental isolates (Muc504-1 and Muc489-1) that harbored an identical high-impact mutation with the *SXI1*α gene, suggesting a highly conserved nature and potential functional importance of *SXI1*α that is yet to be characterized. Further studies are needed to clarify the downstream regulators involved in this novel repression role of Sxi1α.

In *S. cerevisiae*, the *MAT*α2 transcription factor functions both as a homodimer and heterodimer with *MAT***a**1, playing key roles in mating-type regulation (Keleher et al. 1988; Herskowitz 1989; Goutte and Johnson 1993). The transcriptional regulation of **a**-specific and haploid-specific genes involves interactions with the transcription factor Mcm1 (Keleher et al. 1988; Elble and Tye 1991). Given this precedent, a similar dual functionality with/without mating partner may exist for the sex-specific HD

transcription factor Sxi1α in *Cryptococcus*. Our results suggest that Sxi1α might act as both a positive (e.g., in **a** x α mating development) and a negative regulator (e.g., in α x α cell fusion), potentially explaining why our previous result showed that its deletion does not produce a clear phenotype beyond **a** x α crosses (Hull et al. 2004). This phenomenon is reminiscent of the mitogen-activated protein kinase Kss1 in *S. cerevisiae*, which regulates pseudohyphal differentiation through complex signaling mechanisms and functions as a multifunctional regulator in fungal development with counter-balanced positive and negative roles (Madhani et al. 1997).

Taken together, while the HD proteins Sxi1α and Sxi2**a** are dispensable for colony morphology, sporulation, and cell viability during unisexual reproduction, Sxi1α plays a key inhibitory role in both α x α and **a** x α cell fusion, whereas Sxi2**a**'s contributions to this process is unclear. These findings suggest that Sxi1α may have yet to be characterized novel functions during *Cryptococcus* mating that echo those in other well studied fungal species, highlighting the regulatory complexity of sexual reproduction in this important human fungal pathogen.

Data availability

Raw WGS sequencing reads have been deposited in Bioproject: PRJNA1219566.

Acknowledgments

We thank Anna Floyd-Averette for constant support, Connor Larmore and Anna Lehmann for critical reading, Dr. Marco Dias Coelho for suggestions on data presentation, Moayad Shehadeh and Dr. Bian Zhuyun for technical support, and all the members of the Heitman Lab for constructive suggestions. We also thank Dr. Xiaorong Lin (University of Georgia) for sharing the XL280 strains, Dr. Ruiyun Zeng (North Carolina State University) for assistance in data visualization, and Dr. Devi Swain Lenz (Duke's Sequencing and Genomic Technologies Core Facility) for advice and expertise.

Funding

This study was supported by NIH/NIAID R01 grants AI039115-27, AI050113-20, and AI133654-07. J. Heitman is co-director and fellow of the Canadian Institute for Advanced Research (CIFAR) program Fungal Kingdom: Threats & Opportunities.

Conflict of Interest

The authors declare no conflicts of interest.

Literature cited

Abramson J, Adler J, Dunger J, Evans R, Green T, Pritzel A, Ronneberger O, Willmore L, Ballard AJ, Bambrick J, et al. 2024. Accurate structure prediction of biomolecular interactions with AlphaFold 3. Nature. 630(8016):493–500. doi:10.1038/s41586-024-07487-w.

Bian Z, Xu Z, Peer A, Choi Y, Priest SJ, Akritidou K, Dasgupta A, Dahlmann TA, Kück U, Nowrousian M, et al. 2024. Essential genes encoded by the mating-type locus of the human fungal pathogen *Cryptococcus neoformans*. doi:10.1101/2024.12.02.626420. [accessed 2025 Feb 4]. http://biorxiv.org/lookup/doi/10.1101/2024.12.02.626420.

Desjardins CA, Giamberardino C, Sykes SM, Yu C-H, Tenor JL, Chen Y, Yang T, Jones AM, Sun S, Haverkamp MR, et al. 2017. Population genomics and the evolution of virulence in the fungal pathogen *Cryptococcus neoformans*. Genome Res. 27(7):1207–1219. doi:10.1101/gr.218727.116.

Dranginis AM. 1990. Binding of yeast al and α2 as a heterodimer to the operator DNA of a haploid-specific gene. Nature. 347(6294):682–685. doi:10.1038/347682a0.

Ekena JL, Stanton BC, Schiebe-Owens JA, Hull CM. 2008. Sexual development in *Cryptococcus neoformans* requires *CLP1* , a target of the homeodomain transcription factors Sxi1α and Sxi2**a**. Eukaryot Cell. 7(1):49–57. doi:10.1128/EC.00377-07.

Elble R, Tye BK. 1991. Both activation and repression of a-mating-type-specific genes in yeast require transcription factor Mcm1. Proc Natl Acad Sci USA. 88(23):10966–10970. doi:10.1073/pnas.88.23.10966.

Fan Y, Lin X. 2018. Multiple applications of a transient CRISPR-Cas9 coupled with electroporation (TRACE) system in the *Cryptococcus neoformans* species complex. Genetics. 208(4):1357–1372. doi:10.1534/genetics.117.300656.

Fu C, Davy A, Holmes S, Sun S, Yadav V, Gusa A, Coelho MA, Heitman J. 2021. Dynamic genome plasticity during unisexual reproduction in the human fungal pathogen *Cryptococcus deneoformans*. Copenhaver GP, editor. PLoS Genet. 17(11):e1009935. doi:10.1371/journal.pgen.1009935.

Gillissen B, Bergemann J, Sandmann C, Schroeer B, Bölker M, Kahmann R. 1992. A two-component regulatory system for self/non-self recognition in *Ustilago maydis*. Cell. 68(4):647–657. doi:10.1016/0092-8674(92)90141-X.

Goutte C, Johnson AD. 1988. a1 Protein alters the dna binding specificity of α2 repressor. Cell. 52(6):875–882. doi:10.1016/0092-8674(88)90429-1.

Goutte C, Johnson AD. 1993. Yeast a1 and α2 homeodomain proteins form a DNA-binding activity with properties distinct from those of either protein. Journal of Molecular Biology. 233(3):359–371. doi:10.1006/jmbi.1993.1517.

Heimel K, Scherer M, Schuler D, Kämper J. 2010. The *Ustilago maydis* Clp1 protein orchestrates pheromone and *b* -dependent signaling pathways to coordinate the cell cycle and pathogenic development. The Plant Cell. 22(8):2908–2922. doi:10.1105/tpc.110.076265.

Herskowitz I. 1989. A regulatory hierarchy for cell specialization in yeast. Nature. 342(6251):749–757. doi:10.1038/342749a0.

Hsueh Y-P, Xue C, Heitman J. 2009. A constitutively active GPCR governs morphogenic transitions in *Cryptococcus neoformans*. EMBO J. 28(9):1220–1233. doi:10.1038/emboj.2009.68.

Huang J, Larmore CJ, Priest SJ, Xu Z, Dietrich FS, Yadav V, Magwene PM, Sun S, Heitman J. 2024. Distinct evolutionary trajectories following loss of RNA interference in *Cryptococcus neoformans*. Proc Natl Acad Sci USA. 121(47):e2416656121. doi:10.1073/pnas.2416656121.

Huang J, Rowe D, Subedi P, Zhang W, Suelter T, Valent B, Cook DE. 2022. CRISPR-Cas12a induced DNA double-strand breaks are repaired by multiple pathways with different mutation profiles in *Magnaporthe oryzae*. Nat Commun. 13(1):7168. doi:10.1038/s41467-022-34736-1.

Huang MY, Joshi MB, Boucher MJ, Lee S, Loza LC, Gaylord EA, Doering TL, Madhani HD. 2022. Short homology-directed repair using optimized Cas9 in the pathogen *Cryptococcus neoformans* enables rapid gene deletion and tagging. Rando O, editor. Genetics. 220(1):iyab180. doi:10.1093/genetics/iyab180.

Hull CM, Boily M-J, Heitman J. 2005. Sex-Specific homeodomain proteins Sxi1α and Sxi2 **a** coordinately regulate sexual development in *Cryptococcus neoformans*. Eukaryot Cell. 4(3):526–535. doi:10.1128/EC.4.3.526-535.2005.

Hull CM, Cox GM, Heitman J. 2004. The α-specific cell identity factor Sxi1α is not required for virulence of *Cryptococcus neoformans*. Infect Immun. 72(6):3643–3645. doi:10.1128/IAI.72.6.3643-3645.2004.

Hull CM, Davidson RC, Heitman J. 2002. Cell identity and sexual development in *Cryptococcus neoformans* are controlled by the mating-type-specific homeodomain protein Sxi1α. Genes Dev. 16(23):3046–3060. doi:10.1101/gad.1041402.

Kämper J, Reichmann M, Romeis T, Bölker M, Kahmann R. 1995. Multiallelic recognition: Nonself-dependent dimerization of the bE and bW homeodomain proteins in *Ustilago maydis*. Cell. 81(1):73–83. doi:10.1016/0092-8674(95)90372-0.

Keleher CA, Goutte C, Johnson AD. 1988. The yeast cell-type-specific repressor α2 acts cooperatively with a non-cell-type-specific protein. Cell. 53(6):927–936. doi:10.1016/S0092-8674(88)90449-7.

Kües U, Göttgens B, Stratmann R, Richardson WV, O'Shea SF, Casselton LA. 1994. A chimeric homeodomain protein causes self-compatibility and constitutive sexual development in the mushroom Coprinus cinereus. EMBO J. 13(17):4054–4059. doi:10.1002/j.1460-2075.1994.tb06722.x.

Kwon-Chung KJ, Bennett JE. 1978. Distribution of alpha and alpha mating types of *Cryptococcus neoformans* among natural and clinical isolates. American Journal of Epidemiology. 108(4):337–340. doi:10.1093/oxfordjournals.aje.a112628.

Li H, Durbin R. 2009. Fast and accurate short read alignment with Burrows–Wheeler transform. Bioinformatics. 25(14):1754–1760. doi:10.1093/bioinformatics/btp324.

Li T. 1998. Crystal structure of the MATa1/MATalpha2 homeodomain heterodimer in complex with DNA containing an A-tract. Nucleic Acids Research. 26(24):5707–5718. doi:10.1093/nar/26.24.5707.

Li T, Stark MR, Johnson AD, Wolberger C. 1995. Crystal structure of the MATa1/MATα2 homeodomain heterodimer bound to DNA. Science. 270(5234):262–269. doi:10.1126/science.270.5234.262.

Lin X, Hull CM, Heitman J. 2005. Sexual reproduction between partners of the same mating type in *Cryptococcus neoformans*. Nature. 434(7036):1017–1021. doi:10.1038/nature03448.

Madhani HD, Styles CA, Fink GR. 1997. MAP kinases with distinct Inhibitory functions impart signaling specificity during yeast differentiation. Cell. 91(5):673–684. doi:10.1016/S0092-8674(00)80454-7.

Martínez CZ, Magwene PM. FungalPop: A biofinformatics pipeline for building population genomic databases for fungal organisms. in prep Funded by NIH R01AI133654.

Mead ME, Stanton BC, Kruzel EK, Hull CM. 2015. Targets of the Sex Inducer homeodomain proteins are required for fungal development and virulence in *Cryptococcus neoformans*. Mol Microbiol. 95(5):804–818. doi:10.1111/mmi.12898.

Meng EC, Goddard TD, Pettersen EF, Couch GS, Pearson ZJ, Morris JH, Ferrin TE. 2023. UCSF ChimeraX : Tools for structure building and analysis. Protein Science. 32(11):e4792. doi:10.1002/pro.4792.

Phadke SS, Feretzaki M, Heitman J. 2013. Unisexual reproduction enhances fungal competitiveness bypromoting habitat exploration via hyphal growth and sporulation. Eukaryot Cell. 12(8):1155–1159. doi:10.1128/EC.00147-13.

Roth C, Sun S, Billmyre RB, Heitman J, Magwene PM. 2018. A high-resolution map of meiotic recombination in *Cryptococcus deneoformans* demonstrates decreased recombination in unisexual reproduction. Genetics. 209(2):567–578. doi:10.1534/genetics.118.300996.

Sun S, Billmyre RB, Mieczkowski PA, Heitman J. 2014. Unisexual reproduction drives meiotic recombination and phenotypic and karyotypic plasticity in *Cryptococcus neoformans*. Butler G, editor. PLoS Genet. 10(12):e1004849. doi:10.1371/journal.pgen.1004849.

Sun S, Coelho MA, David-Palma M, Priest SJ, Heitman J. 2019. The evolution of sexual reproduction and the mating-type Locus: links to pathogenesis of *Cryptococcus* human pathogenic fungi. Annu Rev Genet. 53(1):417–444. doi:10.1146/annurev-genet-120116-024755.

Sun S, Fu C, Ianiri G, Heitman J. 2020. The pheromone and pheromone receptor mating-type locus is involved in controlling uniparental mitochondrial inheritance in *Cryptococcus*. Genetics. 214(3):703–717. doi:10.1534/genetics.119.302824.

Sun S, Priest SJ, Heitman J. 2019. *Cryptococcus neoformans* mating and genetic Crosses. Current Protocols in Microbiology. 53(1):e75. doi:10.1002/cpmc.75.

Vollmeister E, Schipper K, Baumann S, Haag C, Pohlmann T, Stock J, Feldbrügge M. 2012. Fungal development of the plant pathogen *Ustilago maydis*. FEMS Microbiol Rev. 36(1):59–77. doi:10.1111/j.1574-6976.2011.00296.x.

Wahl R, Zahiri A, KÃ¤mper J. 2010. The *Ustilago maydis b* mating type locus controls hyphal proliferation and expression of secreted virulence factors *in planta*. Molecular Microbiology. 75(1):208–220. doi:10.1111/j.1365-2958.2009.06984.x.

Xue C, Tada Y, Dong X, Heitman J. 2007. The human fungal pathogen *Cryptococcus* can complete its sexual cycle during a pathogenic association with plants. Cell Host & Microbe. 1(4):263–273. doi:10.1016/j.chom.2007.05.005.

Yadav V, Sun S, Heitman J. 2023. On the evolution of variation in sexual reproduction through the prism of eukaryotic microbes. Proc Natl Acad Sci USA. 120(10):e2219120120. doi:10.1073/pnas.2219120120.

Yan Z, Hull CM, Heitman J, Sun S, Xu J. 2004. SXI1α controls uniparental mitochondrial inheritance in *Cryptococcus neoformans*. Current Biology. 14(18):R743–R744. doi:10.1016/j.cub.2004.09.008.

Zhai B, Zhu P, Foyle D, Upadhyay S, Idnurm A, Lin X. 2013. Congenic strains of the filamentous form of *Cryptococcus neoformans* for studies of fungal morphogenesis and virulence. Infect Immun. 81(7):2626–2637. doi:10.1128/IAI.00259-13.

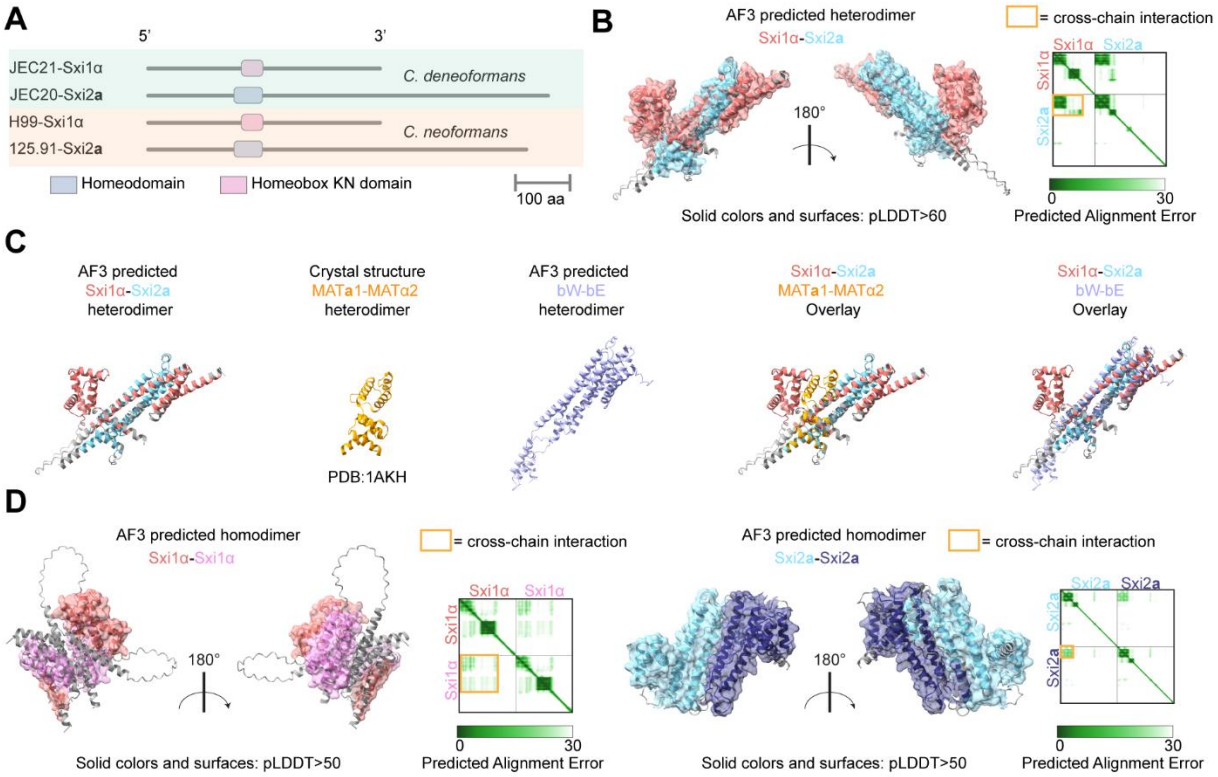

Figure 1. AlphaFold3 predicted heterodimer and homodimers of Sxi1α and Sxi2a.

(A) Predicted domain structures of Sxi1α and Sxi2**a** in *C. neoformans* and *C. deneoformans*. (B) AlphaFold3 (AF3)-predicted heterodimer structure of Sxi1α and Sxi2**a** from *C. deneoformans* JEC21 and JEC20. C-terminal disordered regions were hidden for visualization. Only regions with a predicted local distance difference test (pLDDT) score >60 were colored and surfaced. The predicted alignment error (PAE) plot of the predicted Sxi1α-Sxi2**a** heterodimer is displayed in the right panel. (C) Overlay of AlphaFold3-predicted Sxi1α-Sxi2**a** heterodimer with crystal structure of MAT**a**1-MATα2 (from *S. cerevisiae*, PDB:1AKH) and predicted bW-bE heterodimer (from *U. maydis*, with high confidence ipTM = 0.74 pTM = 0.64). Pairing was performed with the "Matchmaker" function in Chimera X. (D) AlphaFold3-predicted homodimer structures with PAE plots for Sxi1α-Sxi1α (left panel) and Sxi2**a**-Sxi2**a** (right panel). Only regions with a pLDDT score >50 were colored and surfaced.

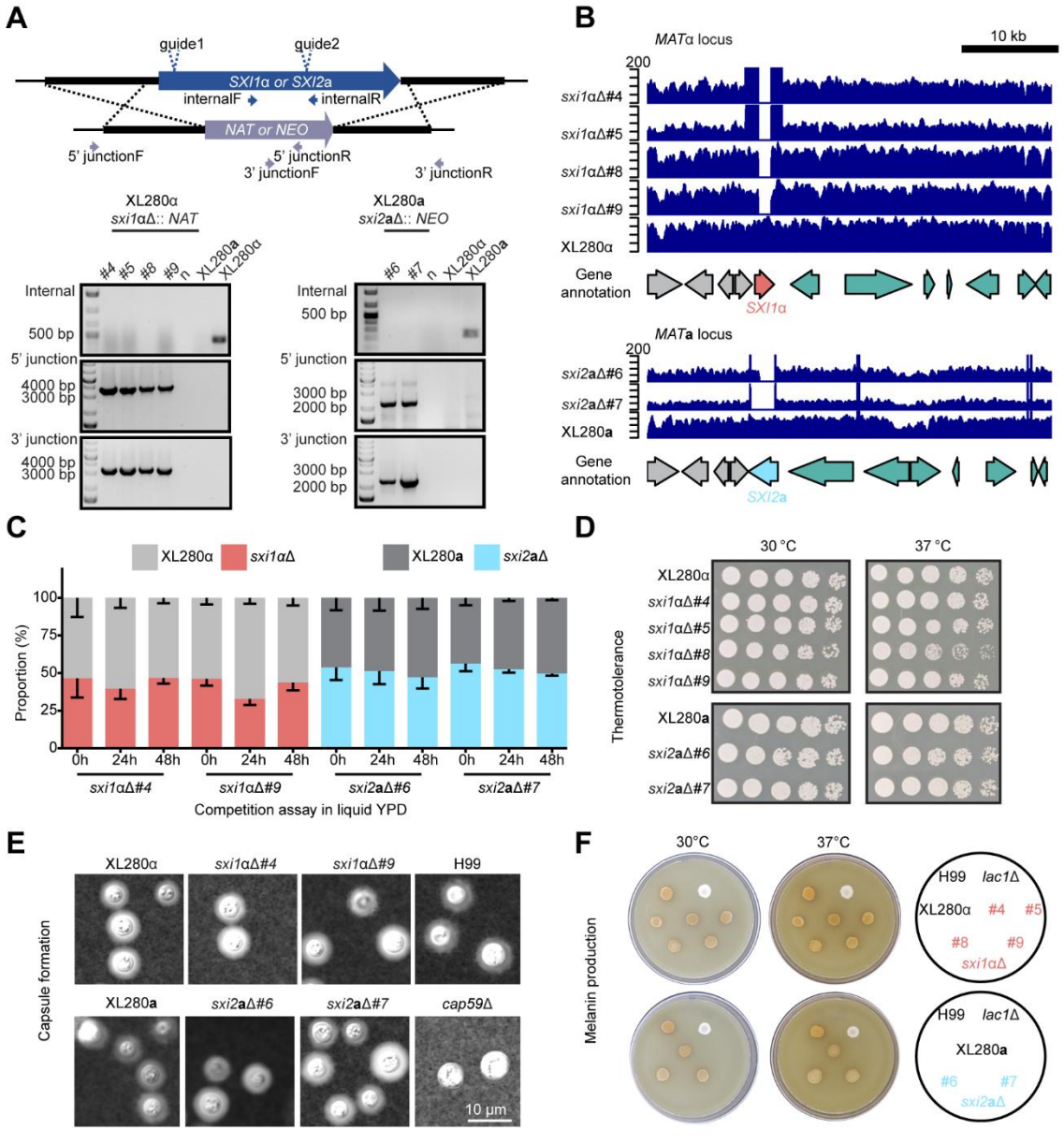

Figure 2. Sxi1α and Sxi2a are not involved in growth, capsule formation and melanin production.

(A) Generation of *sxi1*αΔ and *sxi2***a**Δ mutants in XL280α and XL280**a**, respectively. Transformants were verified through internal PCR targeting the ORF, along with 5' and 3' junction PCRs specific to the drug resistance marker to confirm proper integration at the genomic locus. (B) Whole-genome sequencing (WGS) reads mapping confirming the complete or partial deletion of *SXI1*α and *SXI2***a**. Genes located outside or inside the mating-type locus are labeled gray and green, respectively, with *SXI1*α labeled red and *SXI2***a** blue. (C) *In vitro* competition assays between *sxi1*αΔ and *sxi2***a**Δ mutants, each carrying either the *NAT* or *NEO* resistance markers, and the corresponding XL280 wildtype strains. The assay was

performed in liquid YPD with four independent replicates after 0, 24, and 48 h of incubation. Error bars indicate standard deviation. (D) Serial dilutions of *sxi1*α**Δ** and *sxi2***a****Δ** mutants, along with the corresponding XL280 wildtype strains, were spotted on solid YPD media and incubated at 30°C and 37°C. (E) Saturated cultures of the indicated strains, grown in RPMI medium, were stained with India ink to visualize capsule formation. The H99 strain and isogenic *cap59***Δ** mutant served as positive and negative controls, respectively. (F) Overnight cultures of the indicated strains were spotted on Niger seed medium to monitor melanin formation. The H99 strain and isogenic *lac1***Δ** mutant served as positive and negative controls, respectively.

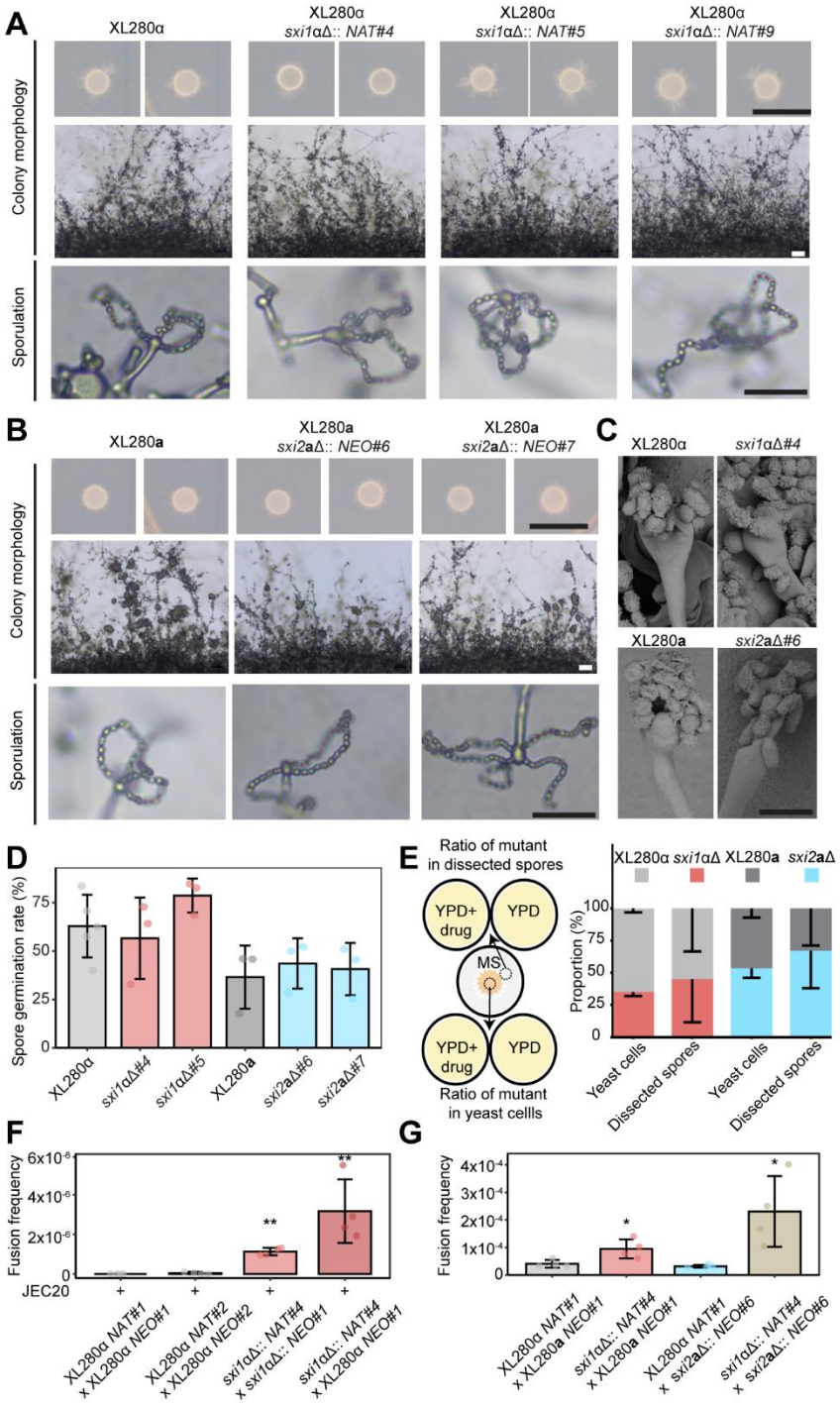

Figure 3. Sxi1α and Sxi2a are not required for hyphal growth or basidium and spore production but are important for cell-cell fusion.

(A and B) Colony morphology, self-filamentation, and sporulation phenotypes of independent *sxi1*αΔ (A) and *sxi2***a**Δ (B) mutants on MS media. Scale bars, 1 cm (upper panel), 100 μm (middle panel) and 20 μm (bottom panel). (C) Scanning electron microscopy (SEM) analysis of basidia and basidiospores from the

indicated solo-culture on MS media. Samples were grown on MS media for 1 to 2 weeks before microscopy. Scale bar: 5 μm. (D) Germination rate of random spores dissected from the indicated solo-cultures. At least 3 replicates were performed for each strain (indicated by dots). The height of the bar indicates the mean and error bars depict the standard deviation among the replicates. (E) Competition assays between *sxi1*αΔ, *sxi2***a**Δ mutants, each carrying either the *NAT* or *NEO* resistance marker, and the corresponding XL280 wildtype strain. The assay was performed on MS medium. Spores at the periphery were dissected and transferred to drug plates to measure the presence of the mutants. Internal yeast cells were counted for normalization. Five different spots were analyzed for each competition. (F) Frequency of α x α fusion for the indicated mating with the assistance of JEC20. Cells from the indicated mating assay on V8 agar (pH = 7.0) for 72 h were plated on YPD + NAT + G418 and YPD to determine the ratio of cell-cell fusion products in the population. ** indicates p-value < 0.01 by using an unpaired student t-test. (G) Frequency of **a** x α fusion for the indicated crosses. Cells from the indicated mating assays on V8 agar (pH=7.0) for 48 h were plated on YPD+NAT+G418 and YPD to determine the ratio of cell-cell fusion products in the population. * Indicates p-value < 0.05 by using an unpaired student t-test.